Optimal and centralized reservoir management for drought and flood protection on the upper Seine-Aube river system using stochastic dual dynamic programming

Raso, L.; Chiavico, M.; Dorchies, D.

DOI
10.1061/(ASCE)WR.1943-5452.0001040

Publication date
2019

Document Version
Final published version

Published in
Journal of Water Resources Planning and Management

Optimal and Centralized Reservoir Management for Drought and Flood Protection on the Upper Seine–Aube River System Using Stochastic Dual Dynamic Programming

L. Raso, Ph.D.[1]; M. Chiavico[2]; and D. Dorchies[3]

Abstract: The basin of the Seine River is an extremely important economic region for France and Europe. Four reservoirs are operated to reduce the natural variability of the Seine River, reducing both flood and drought risk. Presently, reservoir operation is not centrally coordinated, and release rules are based on empirical rule curves. This study presents the setting of an optimal and centralized solution to the problem of reservoir operation on the Upper Seine–Aube river system, found by applying the stochastic dual dynamic programming (SDDP) procedure. The novelty of this study lies on the combination of reservoir and hydraulic models in SDDP for flood and drought protection. Including the hydraulic process in SDDP is required for estimating flood and drought at different locations along the river, and for representing the delay between the release from the reservoirs and their effects downstream. The study case covers the Seine basin until the confluence with the Aube River: this system includes two reservoirs, the city of Troyes, France, and, at the confluence of the two rivers, the nuclear power plant at Nogent-Sur-Seine. Results shows that the SDDP solution can be effectively used to optimize the operation of a water system made of multiple reservoirs and multiple hydraulic transfer components, solving a relatively large stochastic dynamic programming problem in an acceptable time. The management obtained from SDDP rules exploits the centralized operation and, compared to the current operational rules, results in more frequent but shorter, less intense, and less severe flood and drought events at Nogent-Sur-Seine.
DOI: 10.1061/(ASCE)WR.1943-5452.0001040.

Author keywords: Reservoir operation; Multireservoir systems; Seine river; Stochastic dual dynamic programming; Flood and drought risk.

Introduction

The Upper Seine and the Aube basins extend 8,000 km^2 in total. The Upper Seine and Aube rivers have their source in the same mountain system (Plateau de Langres); their basins are located in northeastern France and are part of the Seine River basin. In the Seine River, the flow regime is characterized by low flows in summer and high flows in winter (Ducharne et al. 2007). The average discharge at the outlet point, i.e., at Nogent-sur-Seine, is about 100 m^3/s. Because of the gentle slope of the Seine Valley, the two rivers have numerous meanders and a slow water runoff.

The Seine River is an extremely important economic region for France and Europe: 20 million people live in the Paris metropolitan area, and the gross domestic product (GDP) is about €600 billion, corresponding to 19% of the national population and to 31% of the national GDP (Ducharne et al. 2007). The presence of cities and industries is the cause of vulnerability to droughts and floods. Regarding droughts, the Seine River provides drinking water to the Paris metropolitan area, including a large number of factories, and is a major agricultural and tourist region (Dorchies et al. 2014). An extreme drought can potentially damage the functioning of the power plant at Nogent-sur-Seine because of the switching-off risk caused by the lack of cooling water flow. Regarding floods, a repeat of the scale of the historically high flooding in Paris in 1910 could affect up to 5 million people today and cause up to €30 billion worth of damage (Baubion 2015).

Four reservoirs, constructed between the 1950s and the 1990s, regulate the discharge on the Seine River, with the main objectives of reducing both floods and droughts. This system of reservoirs is operated by Seine Grands Lacs, a French public institution. Two of these reservoirs, the Aube and the Seine reservoirs, are located in the system under study. Fig. 1 shows the topology of the Upper Seine–Aube River system, including the hydrological catchments, the reservoirs, and the river topology until confluence point at Nogent-sur-Seine.

Currently, each reservoir is operated independently from the others, following a rule curve (RC) that sets the target reservoir volume for each day of the year. The RCs are empirically designed in order to store water during the high-flow season (from November to June), while maintaining adequate flood control volumes, and to sustain low flows during the dry season (from July to October).

The empirical nature of rule curves and the decentralized management of the reservoirs motivated different research studies, aimed at improving the reservoir operation of the Seine River system. Dorchies et al. (2014) evaluated the impacts of predicted climate change on flood and drought risk, and how an adaptive reservoirs management could respond to it. That study, however, did not analyze the potential advantage that a centralized reservoir management could offer. In Ficchì et al. (2015), the application of

[1]Dept. of Multi-Actor Systems, Delft Univ. of Technology, Jaffalaan 5, Delft 2628 BX, Netherlands (corresponding author). Email: l.raso@tudelft.nl; l.n.m.m.raso@gmail.com

[2]Eni, Piazza Ezio Vanoni, 1, San Donato Milanese, MI 20097, Italy.

[3]Irstea, UMR G-EAU, 361 rue Jean-François Breton, BP 5095, 34196 Montpellier Cedex 5, France.

Note. This manuscript was submitted on March 1, 2018; approved on August 31, 2018; published online on January 4, 2019. Discussion period open until June 4, 2019; separate discussions must be submitted for individual papers. This paper is part of the ***Journal of Water Resources Planning and Management***, © ASCE, ISSN 0733-9496.

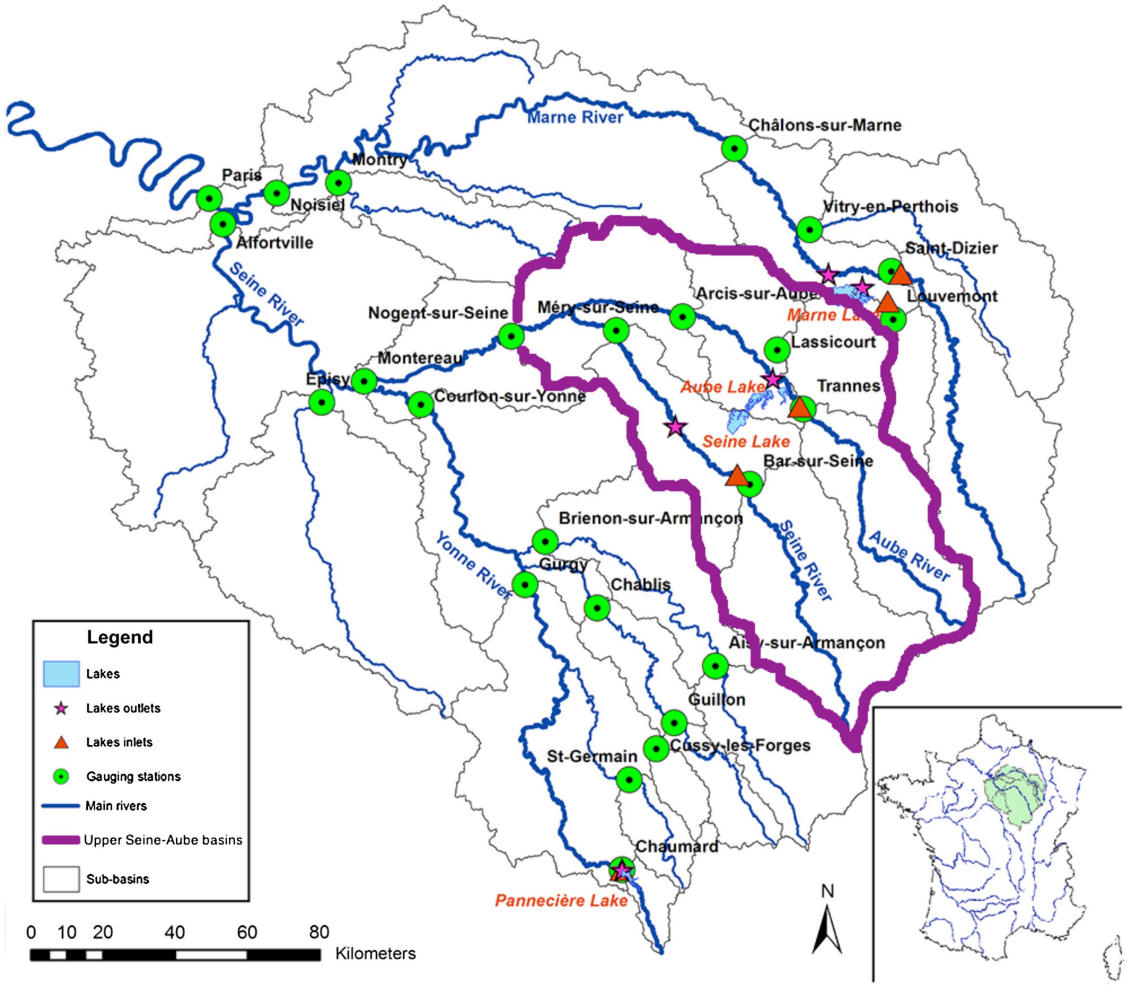

Fig. 1. Seine River basin, including the Upper Seine–Aube River basin.

model predictive control (MPC) (van Overloop 2006) and tree-based model predictive control (TB-MPC) (Raso et al. 2014) showed how an anticipatory and centralized control can improve the level of flood protection on this river. Both MPC and TB-MPC, however, optimize the daily reservoir releases on a 10-day-ahead forecast: the short-term optimization leads to a remarkable improvement in flood protection, but with little effectiveness in reducing drought risk. Drought, in fact, is a slow process that requires a longer horizon. The motivation for the present study stems from the idea that solving an optimal long-term optimization problem can indicate an integrated solution for the Seine reservoir system, able to guarantee flood and drought protection (Castelletti et al. 2008).

The optimal stochastic long-term reservoir operation problem has been solved by employing stochastic dynamic programming (SDP) (Stedinger et al. 1984), and, more recently, by direct policy search (DPS) (Giuliani et al. 2015). Despite the advantages of both SDP and DPS, their applicability to a system made of a large number of variables could be largely inefficient. SDP, in fact, is affected by the so-called curse of dimensionality, which limits its application to small systems, made of few variables (Stedinger et al. 1984; Trezos and Yeh 1987), and DPS, to our knowledge, has not been tested on a system made of tens of states. This study, in fact, intends to include the hydraulic transfer process in the system model. The hydraulic process is represented by a hydraulic model that includes delay and attenuation mechanisms, largely increasing the dimension of the problem.

Stochastic dual dynamic programming (SDDP) (Pereira and Pinto 1985, 1991; Shapiro 2011) is a method derived from SDP that largely attenuates the curse of dimensionality. In the field of water resources management, SDDP has been often used for reservoir operation at the monthly scale, mostly for hydropower scheduling and irrigation supply (Goor et al. 2010; Tilmant et al. 2008, 2009, 2012; Guan et al. 2017; Marques and Tilmant 2018). This study tests how SDDP can offer a centralized and optimal solution to long-term operation of a reservoir-river system, such that both flood and drought protection on the Upper Seine–Aube River system can be improved. The novelty of this study lies on the combination of reservoir and hydraulic models in SDDP for flood and drought protection problems. Including the hydraulic process in SDDP is required for estimating impacts at different locations along the river, and for representing the delay between the release decision and the impacts downstream. The hydrological conditions on this river can pass from median to extreme in about 2 weeks, whereas the travel time from the reservoirs to the system outlet is slightly less than 1 week; therefore, the discharge at the outlet point is only partially controllable by the reservoir releases. The goal of this research is to analyze (i) the capacity of SDDP in finding optimal reservoir operational rules for flood and drought protection on a system model that includes spatial distribution of inflow and hydraulic processes, and (ii) the extent to which SDDP improves the performances of reservoir operational rules with respect to the current management.

J. Water Resour. Plann. Manage., 2019, 145(3): 05019002

The paper is structured as follows: The "Data, Objectives, and Model" section describes the data sets used in this study, the makeup of the cost function used in the optimization, all the components of the system model, and the optimization procedure. The "Results" section presents the outcomes of the optimization experiment, comparing them to the current management and to the natural system. The "Conclusions" section provides the authors' interpretation and other comments on this study.

Data, Objectives, and Model

Data

In the context of the ClimAware project (Dorchies et al. 2014, 2016), Seine Grands Lacs provided data and information on the reservoirs management, specifically (i) the current management rules, expressed as objective RCs; (ii) the thresholds for environmental and reference flows; and (iii) the reservoir and inlet and outlet channel capacities. As a result of the ClimAware project, Irstea Montpellier provided (i) a database of discharge time series, at every control and gauging station, for the 1961–2009 period; (ii) a simulation of the current reservoir management for the 1961–1991 period; and (iii) parameters of the hydraulic model along the watercourses.

Objective Functions

The time-step objective function used in the SDDP procedure is made of (stepwise) linear cost functions. The function is a cost, hence it is to be minimized, and it is the aggregation of different objectives and stations, weighted according to the assigned priority. The following presents the makeup of cost function for each objective, and the weights that define the relative priority for each objective and station.

Floods and Droughts

The flow was monitored at different stations downstream of the lakes. The monitoring stations and their thresholds are presented in Table 1. On each of the gauging stations, flow thresholds defined critical low and high flows. For low flows, thresholds were defined from local decree corresponding to restrictions on the water uses (Arrêté cadre sécheresse, N° 2012 094-0001, Préfet de la Région D'ile-De-France). For high flows, the thresholds corresponded to three critical levels: limit of flooding, flooding in regular area, and exceptional flooding. The reinforced alert threshold was not considered here because of its closeness to the crisis threshold value, and vigilance and limit of flooding thresholds were not considered because their mere informative importance does not imply either direct or indirect damages.

Table 1. Thresholds for monitoring stations

Thresholds	Arcis-sur-Aube	Mery-sur-Seine	Nogent-sur-Seine
Drought thresholds (m^3/s)			
Vigilance	6.3	7.3	25
Alert	**5**	**5**	**20**
Reinforced alert	4	4	17
Crisis	**3.5**	**3.5**	**16**
Flood thresholds (m^3/s)			
Limit	110	140	180
Regular	**260**	**170**	**280**
Exceptional	**400**	**400**	**420**

Note: Bold values were included in the step-cost function of the SDDP problem.

The total cost function was made of separable step-cost functions. The step-cost functions for flood and drought were defined as directly proportional to thresholds exceeding volume, defined as in Eq. (1)

$$g_t^{i,F} = w_{i,j}^F (q_t^i - \bar{q}_t^{Fi,j})^+ \tag{1a}$$

$$g_t^{i,D} = w_{i,j}^D (\bar{q}_t^{Di,j} - q_t^i)^+ \tag{1b}$$

In Eq. (1), t is the time index, i is the station index, and j the type of event index (either regular or extreme), $w_{i,j}^F$ and $w_{i,j}^D$ are the weight for flood and drought events for event j at station i, q_t^i is the discharge at a given station and time, $\bar{q}_t^{Fi,j}$ and $\bar{q}_t^{Di,j}$ are the flood and the drought thresholds for event j at station i, and the $()^+$ operator gives the maximum value between its argument and zero. Step-cost functions for flood and droughts were calculated at the stations of Mary-sur-Seine, Arcis-sur-Aube, and Nogent-sur-Seine.

Different weights should be assigned per type of flood and drought, and for regular and exceptional event. In an economic-rationality approach, each weight should be proportional to the cost of the respective event. Information about real costs of flood and drought or of regular and exceptional events were not available; therefore, weights were assigned according to a priority criterion, where the volume deficit in regular drought events was weighted 1, flood events were weighted 10 times the volume deficits in drought events, and exceptional flood and drought events were weighted 100 times their respective regular events.

Ecology and Lakes Life Quality

The minimum environmental flows (*débit réservé*) require the discharge to be larger than 2 m^3/s for the Aube River and 3 m^3/s for the Seine River. Withdrawing water from the rivers should not reduce the flow below these values. To include this condition, the minimum environmental flows immediately downstream of the reservoir inlets were treated as a soft constraint. The soft constraints on minimum environmental flow used the same step-cost function and the same weight as the exceptional drought event, measured downstream of the Aube and Seine reservoir inlet.

Empty reservoirs are ecologically sensitive to pollution and carrying capacity diminution. The lakes life quality in the Aube and Seine reservoirs were included by a cost function that decreases linearly with the reservoir volume.

Weight per Objective

The relative weight of each station was based on its priority. The assignment of priorities per station and per objective was a subjective choice, based here on a preliminary and general analysis of the system. A more accurate choice would require the involvement of local stakeholders, and the analysis of the interplay between the choice of priorities and overall and local system performances. This type of analysis is a possible followup. This study, however, took the assigned priorities as given.

Nogent-sur-Seine, for its critical challenges such as the protection of both the Parisian metropolitan region and the nuclear power plant, was selected in this study as the highest-priority station. The high-density urban areas predominantly along the Seine River were selected as the second priority; the city of Troyes was the main critical point, together with the Romilly-sur-Seine and Mery-sur-Seine stations. The Aube River, being less urbanized, was considered as having a lower priority with respect to the Seine River, and the protection was limited to the Arcis-sur-Aube station. The last level of priority was given to the lake life quality. Based on this list of priorities, weights were assigned as in Table 2.

Table 2. Weight per station and respective objectives

Station	Priority	Weight	Objective
Aube inlet	II	10	Ecology protection
Arcis-sur-Aube	IV	1	Flood and drought protection
Seine inlet	II	10	Ecology protection
Mery-sur-Seine	III	5	Flood and drought protection (including Troyes)
Nogent-sur-Seine	I	100	Flood and drought protection (including Paris and the nuclear power plant at Nogent-sur-Seine)
Aube reservoir	V	10^{-3}	Lakes life quality
Seine reservoir	V	10^{-3}	Lakes life quality

Model Components

The system under study is composed of six inflows, two off-river reservoirs that withdraw and release water from their river, and a network of two rivers that converge at the confluence point. Fig. 2 shows the topology of the system. The processes relative to (i) the inflows, (ii) the reservoirs, and (iii) the river network are represented by (i) an inflow model, (ii) a reservoir model, and (iii) a hydraulic transfer model. These models are described in the following subsections.

Inflow

The inflow model is a periodic, autoregressive, multivariate model with multiplicative errors:

1. Periodicity is used to represent the seasonal variation of the inflows in terms of mean, standard deviation, and autoregression coefficients.
2. Autoregression is used to represent the autocorrelation of inflows over time.
3. The multivariate feature of the model is used to take into account the spatial cross correlation among inflows.
4. Multiplicative errors are a consequence of class of model used in this study, adapted from Raso et al. (2017). In this class of model, parameters are identified on a transformed signal.

Eq. (2) shows how the transformed signal is defined from the original discharge signal

$$y_t^j = \frac{a_t^j}{\gamma_\tau^j} \tag{2}$$

In Eq. (2), a_t^i is the discharge at station i and time t, and γ_τ^j is the geometric mean of discharge at station j and period τ, the period time index, where τ is the day-of-the-year index, going from 1 to 365, as in Raso et al. (2017).

Table 3 shows that, among some stations, the inflow signals can be very highly correlated. In the literature on streamflow process models (Salas et al. 1982; Bartolini et al. 1988), the correlation among stations is included via the correlation of residuals, i.e., by use of an appropriate covariance matrix of residuals. In this application, however, including correlation via the residuals was insufficient for an adequate reproduction of the long-term correlation among stations.

In order to correctly represent the correlation among stations without having to add state variables, the direct relationship between signals at different stations was included by adding a correlation parameter between coupled correlated stations. For this purpose, stations were divided into main and conditional stations, in which each conditional station was related to a main station. The signal at the conditional stations was considered partially dependent on the signal at the main station. A multivariate additive periodic autoregressive model for the main and conditional stations was identified, as in Salas et al. (1982), and Bartolini et al. (1988), on the transformed signal. The model is represented in Eq. (3)

$$\begin{aligned} y_t^M &= \phi_{\tau,i}^M y_{t-i}^M + \varepsilon_t^M \\ y_t^C &= \alpha y_t^M + \beta_t \\ \text{where } \beta_t &= \phi_{\tau,i}^C \beta_{t-i} + \varepsilon_t^C \end{aligned} \tag{3}$$

In Eq. (3), y_t^M and y_t^C are the transformed signal for the main and the conditional stations; $\phi_{\tau,i}^M$ and $\phi_{\tau,i}^C$ are the autoregressive parameters of the main (M) and conditional (C) stations at period τ; α is the linear regression coefficient between observed y_t^C and

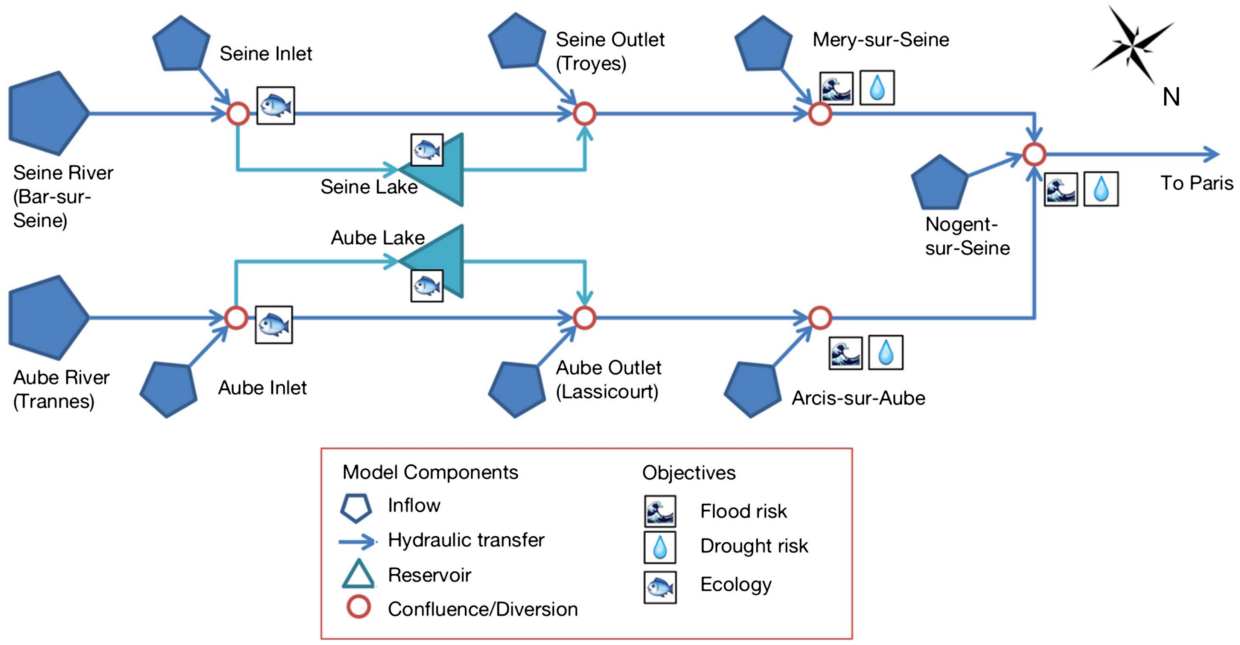

Fig. 2. Topology of the Upper Seine–Aube River system.

J. Water Resour. Plann. Manage., 2019, 145(3): 05019002

Table 3. Correlation coefficient (R^2) among stations

Station	Trannes	Lassicourt	Arcis	Bar	Mery	Nogent
Trannes	1	**0.9304**	0.4874	**0.9445**	0.6608	0.3669
Lassicourt	**0.9304**	1	0.4544	**0.8853**	0.6357	0.3476
Arcis	0.4874	0.4544	1	0.5324	**0.8997**	**0.8741**
Bar	**0.9445**	**0.8853**	0.5324	1	0.7004	0.4133
Mery	0.6608	0.6357	**0.8997**	0.7004	1	**0.8081**
Nogent	0.3669	0.3476	**0.8741**	0.4133	**0.8081**	1

Note: Bold values indicate that the high correlation was included in the model in the determination of main and conditional basins.

y_t^M; β_t, obtained by the relation $\beta_t = y_t^C - \alpha y_t^M$, is the signal on which a multivariate PAR(p) model is identified; and $[\varepsilon_t^M, \varepsilon_t^C] = \varepsilon_t \sim \mathcal{N}(\mu_\tau, \Sigma_\tau)$ is the additive error, where μ_τ and Σ_τ are the mean and covariance matrix of the errors at period τ.

The selection of main and conditional stations was based on the correlation among stations. Table 3 shows the value of the correlation coefficient R^2 among all stations. From Table 3 it emerges that the system is composed by two groups of spatially correlated hydrological discharge: the first group is made of the stations at Trannes, Lassicourt, and Bar-sur-Seine, and the second group is made of the stations at Arcis-sur-Aube, Mery, and Nogent-sur-Seine. The first group corresponds to the basins located in the mountainous area of the Plateau des Langres, and the second corresponds to the basins in the flat area of the Seine Valley. Bar-sur-Seine was selected as the main station for the first group because its mean flow is the largest of all stations. Arcis-sur-Aube was selected as main station for the second group because of its correlation with the other stations.

Once the additive model was identified on the transformed signal, a multiplicative model was defined on the discharge, as in Raso et al. (2017). The model comes in two versions, nonlinear and linearized: the accurate nonlinear version was used in the SDDP forward phase, where the model was simply used to generate a series of inflow, hence no constraints on the model structure were required; the approximate linearized version was used in the SDDP backward phase, where the model was used in the optimization, hence the model has to be linear (Raso et al. 2017). Eq. (4*a*) describes the nonlinear model; Eq. (4*b*) describes its linearized version

$$a_t^j = \kappa_\tau^j \cdot a_{t-i}^{M\varphi_{\tau,i}^{j|M}} \cdot a_{t-i}^{j\phi_{\tau,i}^j} \cdot \xi_t^j \tag{4a}$$

$$\tilde{a}_t^j = (\rho_{\tau,i}^{j|M} a_{t-i}^M + \rho_{\tau,i}^j a_{t-i}^j) \cdot \xi_t^j + \psi_\tau^j \xi_t^j \tag{4b}$$

where

$$\kappa_\tau^j = \frac{\gamma_\tau^j}{(\gamma_{\tau-i}^M)^{\varphi_{\tau,i}^{j|M}} \cdot (\gamma_{\tau-i}^j)^{\phi_{\tau,i}^j}} \tag{4c}$$

$$\xi_t^j \sim \log \mathcal{N}(\mathrm{M}_\tau, \Sigma_\tau) \tag{4d}$$

$$\rho_{\tau,i}^{j|M} = \gamma_\tau^j \frac{\varphi_{\tau,i}^{j|M}}{\gamma_{\tau-i}^M} \tag{4e}$$

$$\rho_{\tau,i}^j = \gamma_\tau^j \frac{\phi_{\tau,i}^j}{\gamma_{\tau-i}^j} \tag{4f}$$

$$\psi_\tau^j = \gamma_\tau^j \left(1 - \sum_i^p \left(\varphi_{\tau,i}^{j|M} + \phi_{\tau,i}^j\right)\right) \tag{4g}$$

In Eq. (4), j is the index of the station, and $j|M$ is the index of the main station; when j is the conditional station, $\varphi_{\tau,i}^{j|M} = \alpha(\phi_{\tau,i}^M - \phi_{\tau,i}^j)$ is the parameter regulating the influence of the discharge at station M on discharge at station j. If a_t^j is itself a main basin, α is zero, then $\varphi_{\tau,i}^{j|M}$ and $\rho_{\tau,i}^{j|M}$ are also zero. The model parameters are identified on historical inflows. The results of the model identification procedure are described in Appendix II.

Reservoir

Eq. (5) describes the reservoir model

$$s_t^i = s_{t-1}^i + \Delta t \cdot (u_t^i - r_t^i) \tag{5a}$$

subject to

$$s_{\min}^i \le s_t^i \le s_{\max}^i \tag{5b}$$

$$0 \le u_t^i \le u_{\max}^i \tag{5c}$$

$$0 \le r_t^i \le r_{\max}^i \tag{5d}$$

In Eq. (5), i identifies the reservoir (Aube or Seine), t is the time index, s_t^i is the volume, u_t^i is the withdrawal from the river, r_t^i is the release decision, and Δt is the time-step length, $s_{\min}^i$ and $s_{\max}^i$ are the minimum and maximum volumes, and $u_{\max}^i$ and $r_{\max}^i$ are the maximum withdrawal and release. Eq. (5*a*) defines the reservoir continuity equation, where, similar to other studies (Ficchì et al. 2015; Dorchies et al. 2014, 2016), evaporation and other losses are neglected. Eqs. (5*b*)–(5*d*) define the physical constraints on volume, inflow, and release. The model is defined for the Aube and Seine reservoirs.

Hydraulic Transfer

The model employed for representing hydraulic transfer along natural watercourses is the linear lag and route (LLR) model, derived from Munier et al. (2014). The derived LLR model is defined in Eq. (6)

$$q_t^d = \sum_i^{n\ \text{branches}} (1 - m_i) q_{t-1}^d + m_i [d_i q_{t-1-n_i}^i + (1 - d_i) q_{t-n_i}^i] \tag{6a}$$

$$q_t^d \ge 0 \tag{6b}$$

In Eq. (6*a*), $q_t^d (\mathrm{m}^3/\mathrm{s})$ is downstream flow at time t; n branches is the total number of upstream branches; $q_t^i (\mathrm{m}^3/\mathrm{s})$ is upstream branch i flow at time t (m^3/s); m_i is the attenuation coefficient of upstream branch i flow, with $m_i \in [0, 1]$; n_i (days) is delay integer part for upstream branch i flow, with $n_i \in [0, \infty]$; and d_i (days) is delay decimal part for upstream branch i flow, with $d_i \in [0, 1]$. The separation between the integer part and the decimal part has been added for working at a daily time step. The model parameters were identified in the ClimAware project. The inequality constraint in Eq. (6*b*) is added to avoid the withdrawals for the reservoirs resulting in negative discharges on the river downstream of the reservoir inlet.

Seven hydraulic transfer models were defined for the following river sections: (i) from the Aube Reservoir inlet to its outlet, (ii) at the point where the outlet of the Aube Reservoir joins the Aube River, (iii) from the point where the outlet of the Aube Reservoir joins the Aube River to the station at Arcis-sur-Aube, (iv) from the Seine Reservoir inlet to its outlet, (v) at the point where the outlet of the Seine Reservoir joins the Seine River, (vi) from the point where the outlet of the Seine Reservoir joins the Seine River to the station at Mery-sur-Seine, and (vii) from the stations at Arcis-sur-Aube

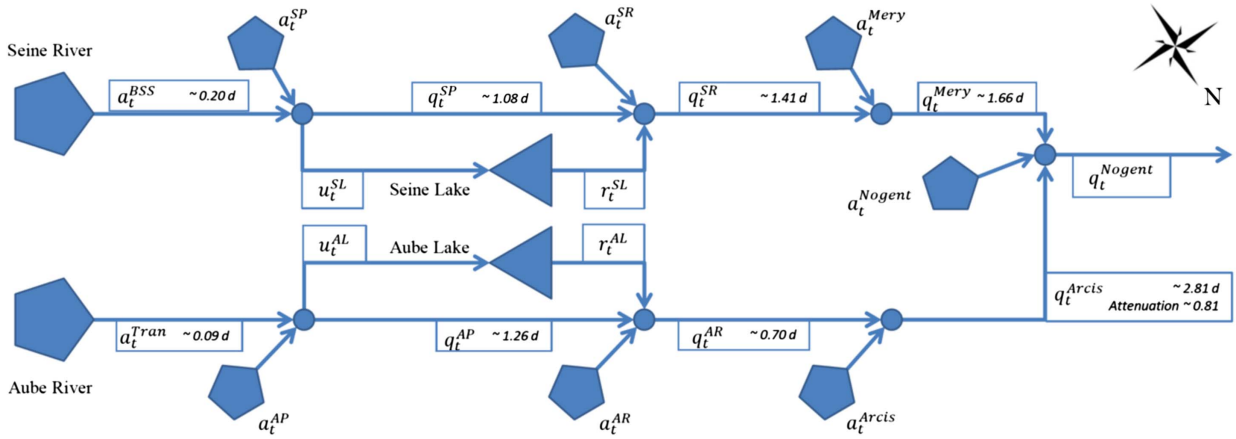

Fig. 3. Hydraulic features of the Seine–Aube River system, with delay coefficient (in days).

and Mery-sur-Seine to the station at Nogent-sur-Seine. The whole hydraulic model is made of 12 state variables: seven hydraulic states plus five additional states to include the delay.

Fig. 3 shows the hydraulic features for the system: for each river branch, the delay coefficient, in days, is presented. The Seine and Aube inlets and releases are assumed to not be affected by delay or attenuation. The Seine River has a slightly superior rate (4.35 days to reach Nogent-sur-Seine) than the Aube River (4.86 days) due to its larger average flow. This difference increases relatively in the part of the system under flow control: after the release stations, the time to reach Nogent-sur-Seine is 3.07 days for the Seine River and 3.51 days for the Aube. The branch from Arcis-sur-Aube to Nogent-sur-Seine stations is the one with highest delay (2.81 days).

Optimization Procedure

The SDDP procedure requires the resolution of the step problem in Eq. (7) for all t in the optimization horizon

$$\min_{u_t, r_t} \mathbb{E}_{\varepsilon}\left[\left(\sum_i g_t^{i,F} + \sum_j g_t^{j,D}\right) + F_t\right] \tag{7}$$

The optimization problem in Eq. (7) is subject to the linear constraints as defined by the system models and the piecewise cost functions. In Eq. (7), $g_t^{i,F}$ and $g_t^{j,D}$ are the time-step cost function for flood and drought events, defined as in Eq. (1); F_t is the approximation of the cost-to-go function; u_t, and r_t are the decision variables, i.e., the intakes and releases from the reservoirs; and $\boldsymbol{\varepsilon}_t$ is the vector of stochastic variables that reproduce the inflow variability. The SDDP problem for the Upper Seine–Aube river system is made of 30 variables, including 20 states and four controls, 20 equality constraints, and 10 inequality constraints. The equations representing the model are detailed in Appendix I.

The SDDP problem was solved on multiple cycles of backward and forward running. The SDDP backward procedure identified the parameters of the additional linear cuts to be added to the cost-to-go function. The SDDP forward procedure instead found the optimal trajectories conditioned to the current approximation of the cost-to-go function (Shapiro 2011). The model time step was set to 1 day, such that the peak of discharge was not lost in a weekly or monthly average operation. The optimization horizon was set to 2 years. The operational rules for the first year were then used in the simulation experiment, whereas the second year was to avoid the cost-to-go function at the end of the optimization horizon (set at zero) influencing the cost-to-go functions of the first year, which were used in the simulation experiment. As for the risk-averse SDDP problem formulation (Shapiro et al. 2013), there is no easy way to define an upper bound for the optimal value of this problem, hence the possibility to define a stopping criteria for SDDP that depends on the chosen level of approximation. For this reason, the stopping criteria was set to an arbitrary number of linear cuts, fixed at 5,000 because it corresponded to a computational time of about 10 h on a Windows PC with a RAM of 4 gigabytes (GB) and a processing speed of 3.70 GHz. The SDDP code is in MATLAB. The optimization software is CPLEX II.

Results

Results were estimated using the historical inflows on a period of 30 years, from August 1, 1961, to July 31, 1991. A set of impact indicators was used to compare performances. The set of impact indicators was made of the return period, $\mathbb{T}_E$; the average event duration, $\mathbb{D}_E$; and the average event intensity, $\mathbb{V}_E$. The return period indicator was inversely proportional to the probability of being in a failure state, and the average event duration and the average event intensity indicators quantify the average features per event. These indicators were closely related to the reliability-resilience-vulnerability indicators (Hashimoto et al. 1982). Indicators were specific to a system failure event of type E. Four types of system failure events were considered: regular flood, exceptional flood, regular drought, and exceptional drought.

Eq. (8) defines the three impact indicators used in this study

$$\mathbb{T}_E = \frac{(\mathbb{P}_E)^{-1}}{T}\left[\frac{\text{years}}{\text{days}}\right] \tag{8a}$$

where $\mathbb{P}_E = \frac{1}{N \cdot T} \cdot \sum_{j=1}^{M} e_j^E \left[\frac{\text{failure days}}{\text{total days}}\right]$

$$\mathbb{D}_E = \frac{1}{M} \cdot \sum_{j=1}^{M} d_j^E \left[\frac{\text{failure days}}{\text{total failure events}}\right] \tag{8b}$$

$$\mathbb{V}_E = \frac{1}{M} \cdot \sum_{j=1}^{M} v_j^E \left[\frac{\text{exceeding discharge}}{\text{total failure events}}\right] \tag{8c}$$

In Eq. (8), j is the event, and E is the type of system failure event. A system failure event happens when the discharge exceeds the threshold for that type of event. Also, N is the simulation horizon [years]; T is the system period, i.e., 365 (days/year);

Station	Event	Natural system (no management)			Current Management			SDDP Optimization		
		Return Period	Average Duration	Average Intensity	Return Period	Average Duration	Average Intensity	Return Period	Average Duration	Average Intensity
ARCIS	Regular Floods	7,5 years / day	2 days	15,1 m3 x 10e5	>30 years / day	0 days	0,0 m3 x 10e5	>30 years / day	0 days	0,0 m3 x 10e5
	Exceptional Floods	>30 years / day	0 days	0,0 m3 x 10e5	>30 years / day	0 days	0,0 m3 x 10e5	>30 years / day	0 days	0,0 m3 x 10e5
	Regular Droughts	0,03 years / day	12,2 days	15,1 m3 x 10e5	0,12 years / day	16,9 days	20,7 m3 x 10e5	0,04 years / day	3,7 days	3,4 m3 x 10e5
	Exceptional Droughts	0,06 years / day	5,9 days	5,4 m3 x 10e5	0,27 years / day	16 days	12,0 m3 x 10e5	0,14 years / day	1,9 days	2,2 m3 x 10e5
MERY	Regular Floods	0,35 years / day	4,8 days	103,9 m3 x 10e5	>30 years / day	0 days	0,0 m3 x 10e5	30 years / day	1 day	2,7 m3 x 10e5
	Exceptional Floods	>30 years / day	0 days	0,0 m3 x 10e5	>30 years / day	0 days	0,0 m3 x 10e5	>30 years / day	0 days	0,0 m3 x 10e5
	Regular Droughts	0,03 years / day	7,7 days	8,2 m3 x 10e5	1,07 years / day	5,6 days	1,0 m3 x 10e5	0,06 years / day	2,5 days	1,8 m3 x 10e5
	Exceptional Droughts	0,09 years / day	4,8 days	3,5 m3 x 10e5	>30 years / day	0 days	0,0 m3 x 10e5	0,46 years / day	1,1 days	2,8 m3 x 10e5
NOGENT	Regular Floods	0,12 years / day	7,2 days	439,9 m3 x 10e5	0,16 years / day	9,2 days	304,5 m3 x 10e5	0,37 years / day	4,5 days	145,2 m3 x 10e5
	Exceptional Floods	0,86 years / day	2,9 days	217,3 m3 x 10e5	>30 years / day	0 days	0,0 m3 x 10e5	>30 years / day	0 days	0,0 m3 x 10e5
	Regular Droughts	0,01 years / day	27,4 days	174,5 m3 x 10e5	0,04 years / day	16,1 days	51,6 m3 x 10e5	0,02 years / day	14,6 days	55,6 m3 x 10e5
	Exceptional Droughts	0,01 years / day	19,3 days	89,9 m3 x 10e5	0,12 years / day	17,9 days	58,1 m3 x 10e5	0,04 years / day	8,2 days	23,1 m3 x 10e5

Best case Intermediate case Worst case

Fig. 4. Results of the simulations.

e_j^E is the occurrence of the jth event of type E; d_j^E is the duration of the jth event of type E (days); v_j^E is the volume that exceeds the threshold for the jth event of type E; and M is the total number of events over the simulation horizon.

The impact indicators were estimated for three alternative reservoir management strategies: natural system, current management, and SDDP optimization. In natural system simulation, impacts were calculated on the naturalized system, as it would be without the reservoirs influence. In current management simulation, impacts were calculated on a simulation using current reservoir operational rules. In SDDP optimization, impacts were calculated on the simulation of centrally optimized management solved by SDDP.

Fig. 4 provides the estimated impacts for the three indicators and the three alternatives (columns), and for the three main stations and the four failure events. From Fig. 4 it emerges that no exceptional flood has occurred in the simulations that include the reservoirs. The lack of extreme events is probably due to the shortness of the time series of observed inflow used in the simulation. The analysis of Fig. 4 shows that the presence of the reservoirs (i.e., simulations corresponding to current management and SDDP optimization) lead to an improvement on almost all indicators. For drought duration and drought intensity indicators, however, the current management performs worse than the natural system. This could be due to the higher priority of flood protection over drought protection in the current reservoir management, in particular on the Aube Reservoir. At the station of Arcis-sur-Aube, the simulations that consider the presence of the reservoirs had no regular flood events, indicating that, after the construction of the Aube Reservoir, flood risk is not a relevant issue at this station.

J. Water Resour. Plann. Manage., 2019, 145(3): 05019002

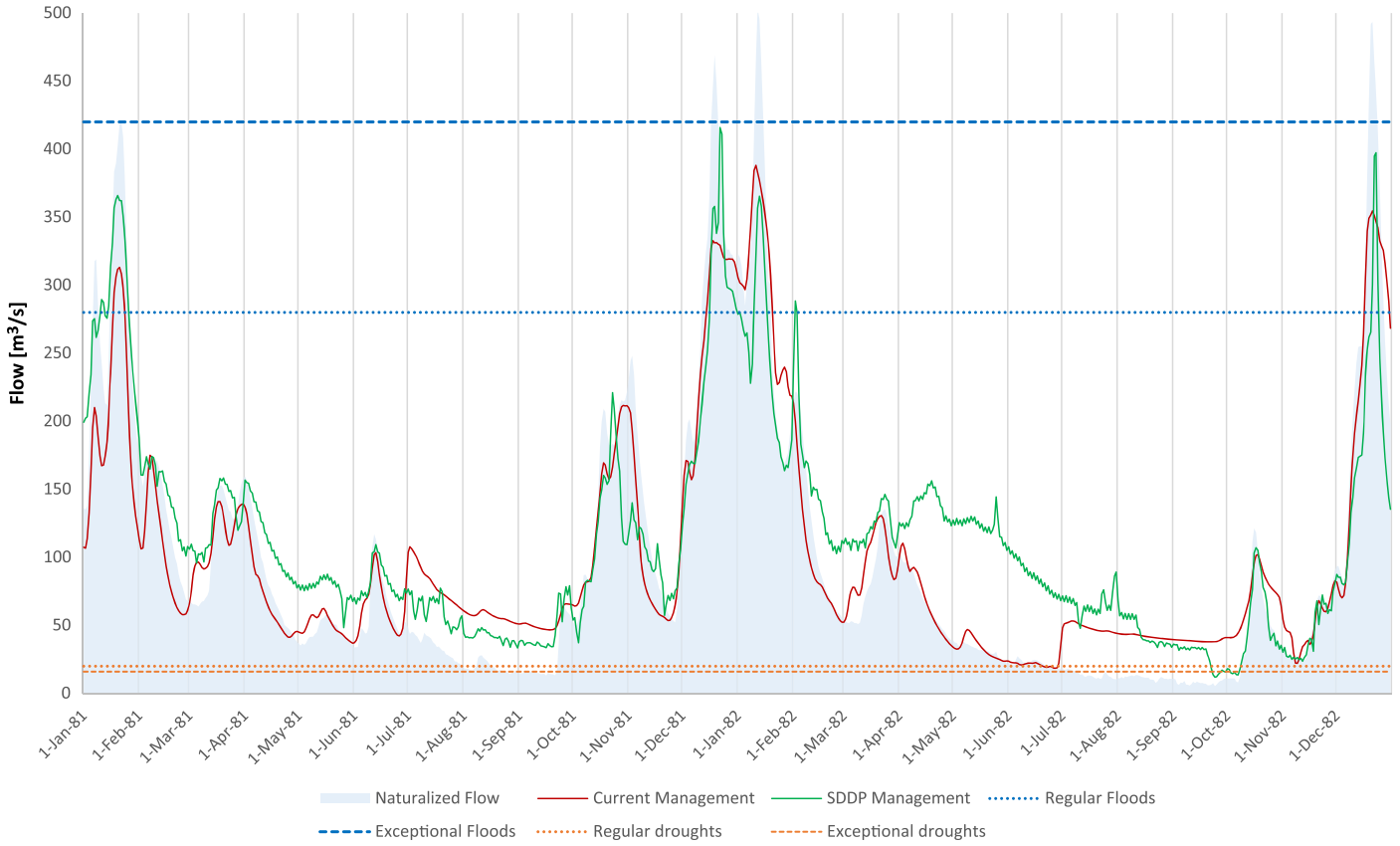

Fig. 5. Seine River at Nogent-sur-Seine station, simulation results for the 1982 flood event.

At the station at Mery-sur-Seine, the SDDP management performs worse for all indicators of regular flood and for most of the indicators related to drought. The worsening at Mery-sur-Seine is counterbalanced by the improvements at the station of Nogent-sur-Seine, where the SDDP management produces better performances on all indicators of regular floods, and generally better performance on indicators related to droughts. This transfer of benefits from Mery-sur-Seine to Nogent-sur-Seine is the effect of the SDDP centralized management: SDDP management favors the protection of the high-priority station at Nogent-sur-Seine, whose cost function has a higher weight, at the cost of local deterioration of performances at the lower-priority station of Mery-sur-Seine.

At the station of Nogent-sur-Seine, the SDDP management produces more frequent and slightly more intense regular droughts than the current management. This slight worsening of performance is counterbalanced by a sensible improvement on indicators for exceptional droughts, for which the SDDP management produces more frequent but shorter and less intense events. The SDDP management in fact favors frequent and short, less intense drought events. We consider the SDDP management as preferable because, in general, more frequent less intense negative events may correspond to a higher resilience (Ciullo et al. 2017). More specifically, our interpretation of the drought policy documents indicates that the most severe consequences of droughts are mostly related to long and intense events (Arrêté cadre sécheresse, N° 2012 094-0001, Préfet de la Région D'ile-De-France).

Fig. 5 presents a detail of simulation results, showing the discharge at Nogent-sur-Seine for the three management scenarios during the 1982 flood events. The 1982 flood event is the major flood event in the simulation period. Fig. 5 shows how the discharge in the SDDP management reaches a higher peak than the discharge for current management. The SDDP in fact minimizes the total volume of water above the regular flood threshold. Within a range of thresholds, the SDDP is independent of the discharge trajectory. If this behavior is considered nonsatisfactory, additional threshold levels can be added in the SDDP cost functions, resulting in a smoother function that better represents the progressivity of damages. Fig. 5 also shows that the discharge trajectory of SDDP management crosses the regular flood threshold multiple times, resulting in multiple small flood events. The trajectory of current management produces a single, long flood event. This, again, is due to the particular form of the SDDP cost function, which must be separable over time. The occurrence of floods that are short and close in time is not always desirable. A penalty on event duration, however, cannot be easily included in SDDP.

Conclusions

This paper presented the application of the SDDP procedure for the optimal and centralized reservoir operation in the Upper Seine–Aube River system, where a system of two reservoirs is operated with the main objectives of flood and drought protection.

The capacity of SDDP to handle large problem has been exploited to model the system at an intermediate level of detail, meaning that the hydraulic processes are included, but in a simplified form. The system model used in SDDP includes (i) the distributed and correlated inflow, represented by a stochastic multivariate autoregressive model; (ii) the hydraulic transfer process, represented by a linear lag and route model; and (iii) the water stocks in reservoirs. Flood and drought risk has been included by use of a piecewise linear cost function. The use of the SDDP technique

gives the solution for the current control problem in a reasonable time. SDDP represent an interesting tool for the design of centralized management in complex water system where flood and drought protection are important objectives.

SDDP centralized management improves the protection of Nogent-sur-Seine, where a nuclear power plant is located, upstream of the urban area of Paris. The station of Nogent-sur-Seine is located at the confluence of the Aube and Upper Seine rivers: its protection requires the coordinate operation of the Aube and Seine Reservoirs. Results of the simulation between SDDP management were compared with the simulated current operational rules and simulated natural system on past conditions. Three features emerged from the analysis of the simulation results. First, the SDDP management increases the flood protection at Nogent-sur-Seine, but at the cost of deteriorating local conditions upstream. The authors consider this a desirable behavior because Nogent-sur-Seine is considered the station with the highest priority. Second, the SDDP management increases the frequency of drought events, but it largely reduces their duration and intensity. This also is a desirable behavior because the considered system is more resilient to frequent, small drought events. Third, regarding droughts, SDDP management hedges risk against extreme events by producing more regular events. This is again a desirable behavior because it exploits the system resilience in facing less intense, more frequent events.

Despite the advantages of using SDDP in tackling this reservoir operation problem, the requirements of SDDP (such as linearity, convexity, and separability) require making several modeling hypotheses that are not always easy to validate: for instance, inflow model complexity is the result of a complex model identification and calibration process, and a trade-off must be found between the quality of the model description and the total amount of computational effort. Moreover, the number of linear cuts has been set to a very large value to ensure the quality of the final results, even if a smaller number of cuts could have improved the computational efficiency of the algorithm. The interplay between performance and number of cuts could be the object of further research. Finally, the selection of weights may look arbitrary, and it has to be chosen in accurate combinations. Further developments of this project could be the extension of the system model to the entire Seine River basin to Paris.

Appendix I. System Model

Variables

Variables	Description	Type
a^{Trann}	Inflow at Trannes	Hydrological model
a^{Lassi}	Inflow at Lassicourt	Hydrological model
a^{Arcis}	Inflow at Arcis-sur-Seine	Hydrological model
a^{BSS}	Inflow at Bar-sur-Seine	Hydrological model
a^{Mery}	Inflow at Mary-sur-Seine	Hydrological model
a^{Nogent}	Inflow at Nogest-sur-Seine	Hydrological model
q^{AP}	Discharge of Aube River after reservoir intake	Hydraulic model
q^{AR}	Discharge of Aube River after reservoir release	Hydraulic model
q^{Arcis}	Discharge at Arcis-sur-Seine	Hydraulic model
q^{SP}	Discharge of Seine River after reservoir intake	Hydraulic model
q^{SR}	Discharge of Seine River after reservoir release	Hydraulic model
q^{Mery}	Discharge at Mery-sur-Seine	Hydraulic model
q^{Nogen}	Discharge at Nogent-sur-Seine	Hydraulic model

Appendix I. (*Continued.*)

Variables	Description	Type
q^{AP1}	Discharge of Aube after intake, additional variable	Hydraulic model
q^{Arcis1}	Discharge at Arcis-sur-Seine, additional variable	Hydraulic model
q^{Arcis2}	Discharge at Arcis-sur-Seine, additional variable	Hydraulic model
q^{SR1}	Discharge of Seine after release, additional variable	Hydraulic model
q^{Mery1}	Discharge at Mery-sur-Seine, additional variable	Hydraulic model
s^{AL}	Volume of Aube Reservoir	Reservoir model
s^{SL}	Volume of Seine Reservoir	Reservoir model
u^{AL}	Intake to Aube Reservoir	Control decision
r^{AL}	Release from Aube Reservoir	Control decision
u^{SL}	Intake to Seine Reservoir	Control decision
r^{SL}	Release from Seine Reservoir	Control decision

Hydrological Model

1. Trannes inflow: Conditional basin

$$a_t^{\text{Tran}} = \xi_t^{\text{Tran}}(\rho_\tau^{\text{Tran}} a_{t-1}^{\text{Tran}}) + \xi_t^{\text{Tran}}(\rho_\tau^{\text{Tran|BSS}} a_{t-1}^{\text{BSS}}) + \xi_t^{\text{Tran}}(\psi_\tau^{\text{Tran}})$$

2. Lassicourt inflow: Conditional basin

$$a_t^{\text{Lassi}} = \xi_t^{\text{Lassi}}(\rho_\tau^{\text{Lassi|BSS}} a_{t-1}^{\text{BSS}}) + \xi_t^{\text{Lassi}}(\rho_\tau^{\text{Lassi}} a_{t-1}^{\text{Lassi}}) + \xi_t^{\text{Lassi}}(\psi_\tau^{\text{Lassi}})$$

3. Arcis-sur-Aube inflow: Main basin

$$a_t^{\text{Arcis}} = \xi_t^{\text{Arcis}}(\rho_\tau^{\text{Arcis}} a_{t-1}^{\text{Arcis}}) + \xi_t^{\text{Arcis}}(\psi_\tau^{\text{Arcis}})$$

4. Bar-sur-Seine inflow: Main basin

$$a_t^{\text{BSS}} = \xi_t^{\text{BSS}}(\rho_\tau^{\text{BSS}} a_{t-1}^{\text{BSS}}) + \xi_t^{\text{BSS}}(\psi_\tau^{\text{BSS}})$$

5. Mery-sur-Seine inflow: Conditioned basin

$$a_t^{\text{Mery}} = \xi_t^{\text{Mery}}(\rho_\tau^{\text{Mery}} a_{t-1}^{\text{Mery}}) + \xi_t^{\text{Mery}}(\rho_\tau^{\text{Mery|Arcis}} a_{t-1}^{\text{Arcis}}) + \xi_t^{\text{Mery}}(\psi_\tau^{\text{Mery}})$$

6. Nogent-sur-Seine inflow: Conditioned basin

$$a_t^{\text{Nogent}} = \xi_t^{\text{Nogent}}(\rho_\tau^{\text{Nogent|Arcis}} a_{t-1}^{\text{Arcis}}) + \xi_t^{\text{Nogent}}(\rho_\tau^{\text{Nogent}} a_{t-1}^{\text{Nogent}}) + \xi_t^{\text{Nogent}}(\psi_\tau^{\text{Nogent}})$$

Hydraulic Models

7. Aube River after intake to Aube Reservoir

$$q_t^{\text{AP}} = d_{\text{AP|Tran}} a_{t-1}^{\text{Tran}} + (1 - d_{\text{AP|Tran}}) a_t^{\text{Tran}} + \alpha^{\text{AP|Arcis}} a_t^{\text{Arcis}} - u_t^{\text{AL}}$$

8. Confluence in Aube release

$$q_t^{\text{AR}} = a_t^{\text{Lassi}} + \alpha^{\text{AR|Arcis}} a_t^{\text{Arcis}} + d_{\text{AR|AP}} q_{t-1}^{\text{AP1}} + (1 - d_{\text{AR|AP}}) q_t^{\text{AP1}} + r_t^{\text{AL}}$$

9. Aube River at Arcis-sur-Aube

$$q_t^{\text{Arcis}} = a_t^{\text{Arcis}} + d_{\text{Arcis|AR}} q_{t-1}^{\text{AR}} + (1 - d_{\text{Arcis|AR}}) q_t^{\text{AR}} - w_\tau^{\text{Arcis}}$$

10. Seine River after intake to Seine Reservoir

$$q_t^{\text{SP}} = d_{\text{SP|BSS}} a_{t-1}^{\text{BSS}} + (1 - d_{\text{SP|BSS}}) a_t^{\text{BSS}} + \alpha^{\text{SP|Mery}} a_t^{\text{Mery}} - u_t^{\text{SL}}$$

11. Confluence in Seine Release

$$q_t^{\mathrm{SR}} = \alpha^{\mathrm{SR|Mery}} a_t^{\mathrm{Mery}} + q_{t-1}^{\mathrm{SP}} + r_t^{\mathrm{SL}}$$

12. Seine River at Mery-Sur-Seine:

$$q_t^{\mathrm{Mery}} = a_t^{\mathrm{Mery}} + d_{\mathrm{Mery|SR}} q_{t-1}^{\mathrm{SR1}} + (1 - d_{\mathrm{Mery|SR}}) q_t^{\mathrm{SR1}}$$

13. Seine and Aube rivers confluence in Nogent-sur-Seine

$$\begin{aligned} q_t^{\mathrm{Nog}} = {} & a_t^{\mathrm{Nog}} + (1 - m_{\mathrm{Nog|Arc}}) q_{t-1}^{\mathrm{Nog}} \\ & + m_{\mathrm{Nog|Arc}} [d_{\mathrm{Nog|Arc}} q_{t-1}^{\mathrm{Arc2}} + (1 - d_{\mathrm{Nog|Arc}}) q_t^{\mathrm{Arc2}}] \\ & + d_{\mathrm{Nog|Mery}} q_{t-1}^{\mathrm{Mery1}} + (1 - d_{\mathrm{Nog|Mery}}) q_t^{\mathrm{Mery1}} - w_\tau^{\mathrm{Nog}} \end{aligned}$$

Hydraulic Model: Additional States

14. $q_t^{\mathrm{AP1}} = q_{t-1}^{\mathrm{AP}}$

15. $q_t^{\mathrm{Arc1}} = q_{t-1}^{\mathrm{Arc}}$

16. $q_t^{\mathrm{Arc2}} = q_{t-1}^{\mathrm{Arc1}}$

17. $q_t^{\mathrm{SR1}} = q_{t-1}^{\mathrm{SR}}$

18. $q_t^{\mathrm{Mery1}} = q_{t-1}^{\mathrm{Mery}}$

Reservoir Models

19. Aube Reservoir

$$s_t^{\mathrm{AL}} = s_{t-1}^{\mathrm{AL}} + u_t^{\mathrm{AL}} - r_t^{\mathrm{AL}}$$

20. Seine Reservoir

$$s_t^{\mathrm{SL}} = s_{t-1}^{\mathrm{SL}} + u_t^{\mathrm{SL}} - r_t^{\mathrm{SL}}$$

Appendix II. Inflow Model Calibration and Testing

Calibration of the inflow model requires the identification of four sets of parameters from discharge data: spatial correlation α_{jM}, autoregression $\phi_{\tau,i}^j$, geometric mean γ_τ^j, and properties of noises log normal distribution, μ_τ and Σ_τ. The first two sets of parameters are obtained by identifying the additive periodic multivariate autoregressive model on the transformed signal; the third set of parameters can be directly derived from data. Properties of the noise's lognormal distribution are calculated on the difference between the linear model and data in order to include linearization correction in an adjusted distribution of noise (which generally has a mean value inferior to unity, to avoid overestimation), such that $\xi_t^j \sim \log \mathcal{N}(E[e_{t\in\tau}^j], \Sigma[e_{t\in\tau}^j])$, where $e_t^j = a_t^{j,\mathrm{observed}} / a_t^{j,\mathrm{linearmodel}}$. Testing the model requires that (i) the model error is white, i.e., uncorrelated in time, and (ii) the model error is distributed as ξ_t. An analysis of these aspects is provided in the following.

Fig. 6 shows the autocorrelation function (ACF) for the hydrological inflows at all stations. From the analysis of Fig. 6 it emerges that the model error is not completely white: lag-1 autocorrelation for the first group of stations (Trannes, Lassicourt, and Bar-sur-Seine) never exceeds 0.3, while the ACF for the second group of stations (Arcis-sur-Aube, Mery, and Nogent-sur-Seine) is very high. The discharges at the second group of stations, however, are not observed data, but derived from the ClimAware project's hydrological model. The hydrological model provided by the ClimAware project suffers from a high slow term error autocorrelation: this can explain the low decay rate of ACF on the Arcis and Nogent-sur-Seine stations. Considering the small contribution of the second group of stations to the total inflow, the autoregression order of these station is considered sufficient for the purpose of this study.

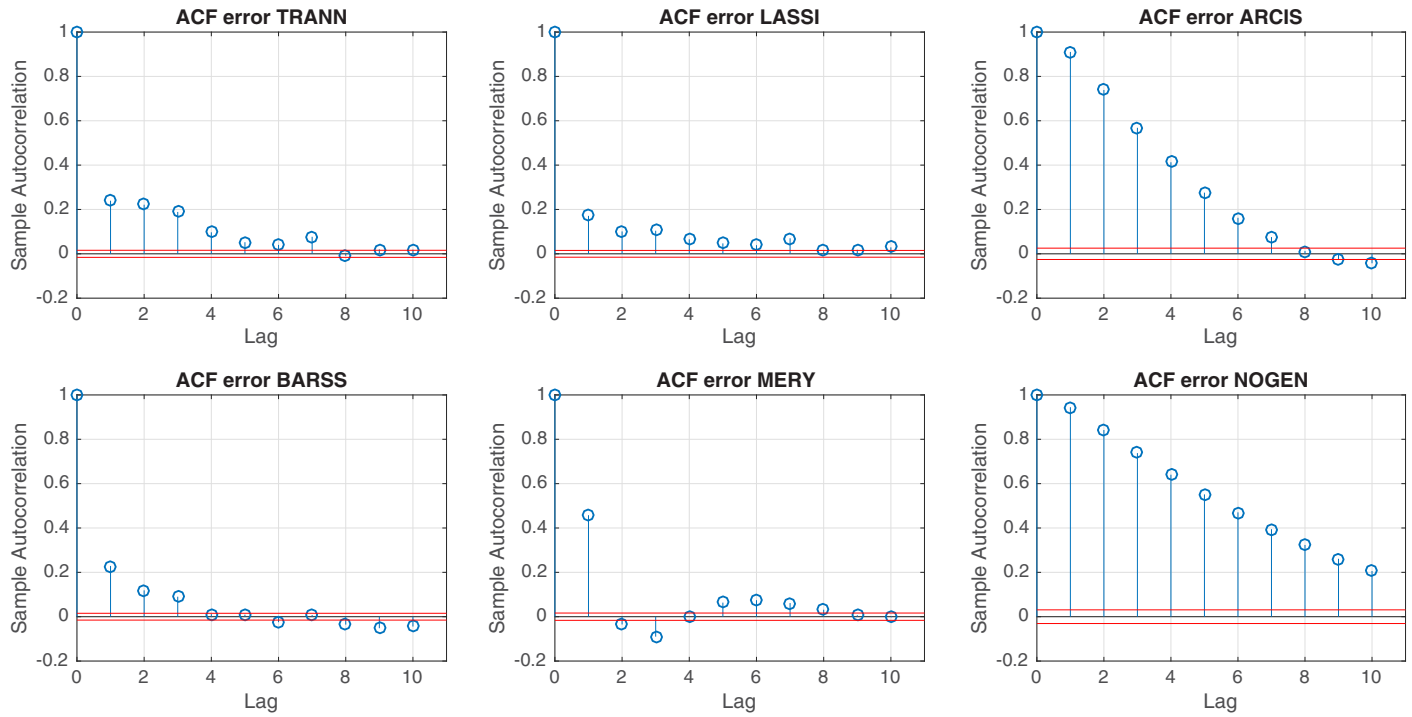

Fig. 6. ACF on model errors.

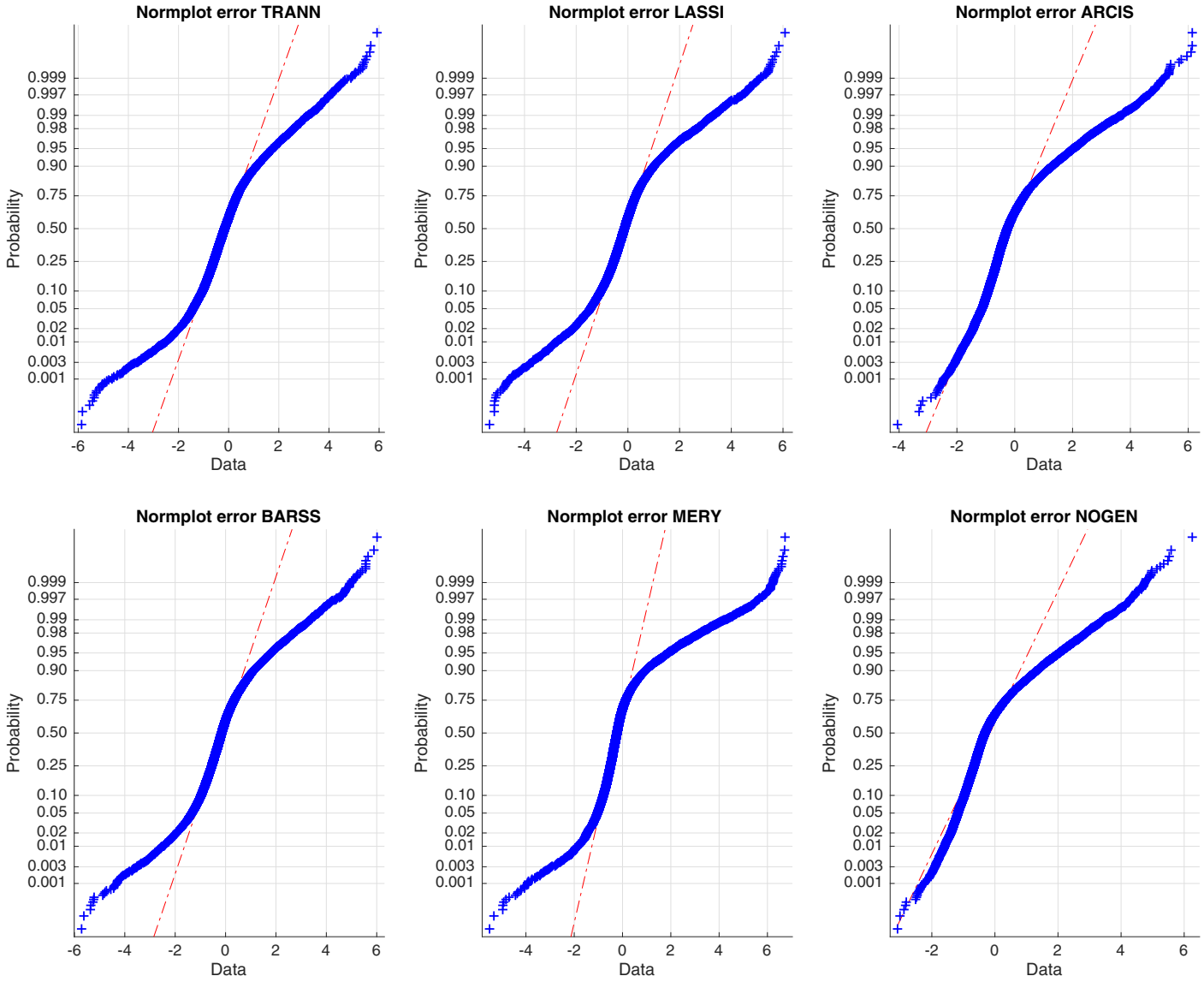

Fig. 7. Normal probability plots on standard logarithmic error distributions.

Observed disturbances should match with the error distribution (i.e., log-normal). Therefore, the logarithm of errors can be compared to a normal distribution. Fig. 7 shows the normal probability plots of the errors at all stations. From Fig. 7, it emerges that the empirical distribution correctly estimates values close to the average, but it underestimates values close to the tails. This problem is particularly evident in the second group of stations (i.e., Arcis-sur-Aube, Mery, and Nogent-sur-Seine).

Acknowledgments

Luciano Raso's research was funded by the AXA Research Fund. Mattia Chiavico's research was funded by the GIS-HED^2 consortium.

References

Bartolini, P., J. D. Salas, and J. T. B. Obeysekera. 1988. "Multivariate periodic ARMA (1, 1) processes." *Water Resour. Res.* 24 (8): 1237–1246. https://doi.org/10.1029/WR024i008p01237.

Baubion, C. 2015. "Losing memory–the risk of a major flood in the Paris region: Improving prevention policies." Supplement, *Water Policy* 17 (S1): 156–179. https://doi.org/10.2166/wp.2015.008.

Castelletti, A., F. Pianosi, and R. Soncini-Sessa. 2008. "Water reservoir control under economic, social and environmental constraints." *Automatica* 44 (6): 1595–1607. https://doi.org/10.1016/j.automatica.2008.03.003.

Ciullo, A., A. Viglione, A. Castellarin, M. Crisci, and G. Di Baldassarre. 2017. "Socio-hydrological modelling of flood-risk dynamics: Comparing the resilience of green and technological systems." *Hydrol. Sci. J.* 62 (6): 880–891. https://doi.org/10.1080/02626667.2016.1273527.

Dorchies, D., et al. 2014. "Climate change impacts on multi-objective reservoir management: Case study on the Seine River basin, France." *Int. J. River Basin Manage.* 12 (3): 265–283. https://doi.org/10.1080/15715124.2013.865636.

Dorchies, D., G. Thirel, C. Perrin, J. C. Bader, R. Thepot, J. L. Rizzoli, C. Jost, and S. Demerliac. 2016. "Climate change impacts on water resources and reservoir management in the Seine river basin (France)." *La Houille Blanche* 5: 32–37. https://doi.org/10.1051/lhb/2016047.

Ducharne, A., et al. 2007. "Long term prospective of the Seine River system: Confronting climatic and direct anthropogenic changes." *Sci. Total Environ.* 375 (1–3): 292–311. https://doi.org/10.1016/j.scitotenv.2006.12.011.

Ficchì, A., L. Raso, D. Dorchies, F. Pianosi, P. O. Malaterre, P. J. Van Overloop, and M. Jay-Allemand. 2015. "Optimal operation of the multireservoir system in the Seine River basin using deterministic and ensemble forecasts." *J. Water Resour. Plann. Manage.* 142 (1): 05015005. https://doi.org/10.1061/(ASCE)WR.1943-5452.0000571.

Giuliani, M., A. Castelletti, F. Pianosi, E. Mason, and P. M. Reed. 2015. "Curses, tradeoffs, and scalable management: Advancing evolutionary multiobjective direct policy search to improve water reservoir operations." *J. Water Resour. Plann. Manage.* 142 (2): 04015050. https://doi.org/10.1061/(ASCE)WR.1943-5452.0000570.

Goor, Q., R. Kelman, and A. Tilmant. 2010. "Optimal multipurpose-multireservoir operation model with variable productivity of hydropower plants." *J. Water Resour. Plann. Manage.* 137 (3): 258–267. https://doi.org/10.1061/(ASCE)WR.1943-5452.0000117.

Guan, Z., Z. Shawwash, and A. Abdalla. 2017. "Using SDDP to develop water-value functions for a multireservoir system with international treaties." *J. Water Resour. Plann. Manage.* 144 (2): 05017021. https://doi.org/10.1061/(ASCE)WR.1943-5452.0000858.

Hashimoto, T., J. R. Stedinger, and D. P. Loucks. 1982. "Reliability, resiliency, and vulnerability criteria for water resource system performance evaluation." *Water Resour. Res.* 18 (1): 14–20. https://doi.org/10.1029/WR018i001p00014.

Marques, G. F., and A. Tilmant. 2018. "Cost distribution of environmental flow demands in a large-scale multireservoir system." *J. Water Resour. Plann. Manage.* 144 (6): 04018024. https://doi.org/10.1061/(ASCE)WR.1943-5452.0000936.

Munier, S., X. Litrico, G. Belaud, and C. Perrin. 2014. "Assimilation of discharge data into semidistributed catchment models for short-term flow forecasting: Case study of the seine river basin." *J. Hydrol. Eng.* 20 (5): 05014021. https://doi.org/10.1061/(ASCE)HE.1943-5584.0001054.

Pereira, M. V. F., and L. M. V. G. Pinto. 1985. "Stochastic optimization of a multireservoir hydroelectric system: A decomposition approach." *Water Resour. Res.* 21 (6): 779–792. https://doi.org/10.1029/WR021i006p00779.

Pereira, M. V. F., and L. M. V. G. Pinto. 1991. "Multi-stage stochastic optimization applied to energy planning." *Math. Program.* 52 (1): 359–375. https://doi.org/10.1007/BF01582895.

Raso, L., P.-O. Malaterre, and J.-C. Bader. 2017. "Effective streamflow process modeling for optimal reservoir operation using stochastic dual dynamic programming." *J. Water Resour. Plann. Manage.* 143 (4): 4017003. https://doi.org/10.1061/(ASCE)WR.1943-5452.0000746.

Raso, L., D. Schwanenberg, N. C. van de Giesen, and P. J. van Overloop. 2014. "Short-term optimal operation of water systems using ensemble forecasts." *Adv. Water Resour.* 71: 200–208. https://doi.org/10.1016/j.advwatres.2014.06.009.

Salas, J. D., D. C. Boes, and R. A. Smith. 1982. "Estimation of ARMA models with seasonal parameters." *Water Resour. Res.* 18 (4): 1006–1010. https://doi.org/10.1029/WR018i004p01006.

Shapiro, A. 2011. "Analysis of stochastic dual dynamic programming method." *Eur. J. Oper. Res.* 209 (1): 63–72. https://doi.org/10.1016/j.ejor.2010.08.007.

Shapiro, A., W. Tekaya, J. P. da Costa, and M. P. Soares. 2013. "Risk neutral and risk averse stochastic dual dynamic programming method." *Eur. J. Oper. Res.* 224 (2): 375–391. https://doi.org/10.1016/j.ejor.2012.08.022.

Stedinger, J. R., B. F. Sule, and D. P. Loucks. 1984. "Stochastic dynamic programming models for reservoir operation optimization." *Water Resour. Res.* 20 (11): 1499–1505. https://doi.org/10.1029/WR020i011p01499.

Tilmant, A., D. Arjoon, and G. F. Marques. 2012. "Economic value of storage in multireservoir systems." *J. Water Resour. Plann. Manage.* 140 (3): 375–383. https://doi.org/10.1061/(ASCE)WR.1943-5452.0000335.

Tilmant, A., Q. Goor, and D. Pinte. 2009. "Agricultural-to-hydropower water transfers: Sharing water and benefits in hydropower-irrigation systems." *Hydrol. Earth Syst. Sci.* 13 (7): 1091–1101. https://doi.org/10.5194/hess-13-1091-2009.

Tilmant, A., D. Pinte, and Q. Goor. 2008. "Assessing marginal water values in multipurpose multireservoir systems via stochastic programming." *Water Resour. Res.* 44 (12): W12431. https://doi.org/10.1029/2008WR007024.

Trezos, T., and W. W. G. Yeh. 1987. "Use of stochastic dynamic programming for reservoir management." *Water Resour. Res.* 23 (6): 983–996.

van Overloop, P.-J. 2006. *Model predictive control on open water systems*. Delft, Netherlands: IOS Press.